JOURNAL OF CATALYSIS **177,** 231–239 (1998)
ARTICLE NO. CA982127

H_2O_2 Oxidation and Epoxidation of Hydrocarbons and Alcohols over Titanium Aluminophosphates TAPO-5, TAPO-11, and TAPO-36

M. Hassan Zahedi-Niaki, Mahendra Parkash Kapoor, and Serge Kaliaguine[1]

Department of Chemical Engineering, Laval University, Ste-Foy, Québec, Canada, G1K 7P4

Received June 23, 1997; revised April 20, 1998; accepted April 28, 1998

Titanium AlPOs, TAPO-5, TAPO-11, and TAPO-36, which have been synthesized hydrothermally, were found to be active in cyclohexane oxyfunctionalization, cyclohexanol and 2-hexanol oxidation, and octene-1 and cyclohexene epoxidation in the presence of dilute hydrogen peroxide. TAPO catalytic oxidation activity was shown to be associated with framework-incorporated Ti atoms and not with any hypothetical Ti species in reaction solution. This activity and H_2O_2 selectivity were in the order TAPO-5 > TAPO-11 > TAPO-36, with TAPO-5 being only slightly less active and selective than a titanium silicalite (TS-1) sample of similar Ti content and higher BET surface area.

Key Words: **titanium aluminophosphate molecular sieves; TAPO-5; TAPO-11; TAPO-36; catalytic oxidation; epoxidation; cyclohexane; cyclohexene; hexanol; cyclohexanol; hydrogen peroxide; H_2O_2 decomposition.**

INTRODUCTION

Aluminophosphate ($AlPO_4$) molecular sieves constitute a class of microporous crystalline inorganic solids similar to zeolites. A variety of structure-type aluminophosphate molecular sieves are reported with a wide diversity of structures (1, 2). The strict alternation of AlO_4^- and PO_4^+ tetrahedra in these materials makes them electronically neutral and therefore comparable to silica polymorphs of zeolites. Isomorphously substituted Ti in such Si polymorphs as titanium silicalites -1 and -2 and titanium -β have remarkable catalytic properties in redox reactions in the presence of dilute hydrogen peroxide (3–5). On the other hand transition metal-substituted aluminophosphate molecular sieves have been reported to be active in oxidation reactions (6–10). In this respect Co-, Cr-, V-, and Fe-containing AlPOs have been more extensively studied than Ti-containing AlPOs.

It is thus of interest to study the substitution of Ti in $AlPO_4$ lattices which provide new environments for the Ti^{4+} cations and potentially a new family of redox catalysts.

[1] To whom correspondence should be addressed. E-mail: kaliagui@gch.ulaval.ca. Fax: (418) 656-5993. Internet: http://www.gch.ulaval.ca/~kaliagui/.

Only a few papers discuss the synthesis of TAPOs (11–13) and still fewer works report their catalytic properties. Ulagappan and Krishnasamy (13) found TAPO-5 and -11 active in phenol hydroxylation. Also some activity was reported for TMAPO-36 (16) and Ti–VPI-5 (10) in catalytic oxidation of cyclohexane to cyclohexanol.

Following our recent report of the synthesis and physicochemical properties of TAPO-5, TAPO-11, and TAPO-36 (12, 15), the present contribution is a systematic comparison of the catalytic properties in liquid phase oxidation of these three TAPOs with those of titanium silicalite-1 (TS-1).

EXPERIMENTAL

Synthesis

The three different titanium aluminophosphate molecular sieves TAPO-5, TAPO-11, and TAPO-36, and one titanium silicalite sample TS-1, were synthesized hydrothermally. The synthesis procedures used in the preparation of TAPO-5 and TAPO-11 are essentially those described by Lok *et al.* (11). TAPO-36 is a new large-pore titanium-containing molecular sieve structurally analogous to AlPO-36. Both were synthesized and reported recently (12, 14). The TS-1 sample was prepared according to the Enichem method (3).

Phosphoric acid (85%, Fisher Scientific Co.) and pseudoboehmite (Vista Chemical Co.) were used as sources for phosphorus and aluminum, respectively. The source of Ti was titanium isopropoxide (Aldrich) for TAPO-5 and titanium (di-isopropoxide) bis (acetylacetonate) (75% sol. in isopropanol, Strem Chemical Co.) for TAPO-11 and TAPO-36.

In a typical TAPO gel preparation phosphoric acid was first diluted with water and to it pseudoboehmite was added. The slurry was stirred continuously until a homogeneous mixture was obtained. Then the titanium-containing reagent was added dropwise to the gel under stirring. After complete homogenization the organic template was added at the rate of 1 ml/min. TPAOH, *n*-Pr_2NH, and Pr_3N were used as template for AFI, AEL, and ATS structure-type

0021-9517/98 $25.00

TABLE 1

Composition and Some Important Properties of the TAPOs and TS-1 Samples

Sample	Structure type	Pore diameter (Å)[a]	Product composition			Specific surface area (m^2/g)[b]	Micropore volume (cm^3/g)[c]
			Al	P	Ti		
TAPO-5	AFI	7.3	0.50	0.49	0.02	305	0.111
AlPO-5			0.49	0.51	—	370	0.147
TAPO-11	AEL	6.3 ∗ 3.9	0.47	0.51	0.02	350	0.074
AlPO-11			0.48	0.52	—	170	0.055
TAPO-36	ATS	7.4 ∗ 6.5	0.48	0.48	0.04	373	0.147
AlPO-36			0.51	0.49	—	370	0.139
TS-1	MFI	5.4 ∗ 5.6	$Si_{0.981}Ti_{0.019}$			480	0.184

[a] From Ref. (2).
[b] Measured by N_2-adsorption.
[c] Determined using *n*-butane adsorption.

materials preparation, respectively. Finally the entire gel was further stirred for at least 30 min. Hydrothermal crystallization was performed in Teflon-coated stainless steel autoclaves under autogeneous pressure and static conditions. Heating duration, temperature, and other details of hydrothermal synthesis are described elsewhere (15). All samples were separated by centrifugation and repeatedly washed with water followed by drying at 353 K for 5 h and calcination at 823 K overnight. Table 1 shows the product composition and some important properties of these materials.

Characterization

As-synthesized and calcined samples were characterized using XRD, bulk chemical analysis (A.A. and ICP), SEM, diffuse reflectance UV–vis spectrometry, N_2 and *n*-butane adsorption, XPS, and ^{27}Al and ^{31}P MAS NMR.

The powder X-ray diffraction spectra were recorded using a Philips pw/1730 X-ray generator with a Ni-filtered Cu$K\alpha$ radiation source and a scintillation counter. Bulk chemical composition was determined using a Jarel–Ash ICP instrument. A Jeol JSM 840A scanning electron microscope was used for micrography. UV–vis spectra were recorded using a Perkin–Elmer lambda 5 spectrometer equipped with diffuse reflectance facility. N_2 adsorption and BET experiments were performed on an OMNISORP 100 instrument. *n*-Butane adsorption capacity was measured using a Perkin–Elmer thermobalance. XPS measurements were conducted in determining elemental surface concentrations and the binding energy of Al_{2p}, P_{2p}, O_{1s}, and $Ti_{2p3/2}$. A V.G. Scientific Escalab Mark II system with a hemispherical analyzer operated in the constant pass energy mode (20 eV) was employed. An Mg$K\alpha$ X-ray source ($h\nu = 1253.6$ eV) was operated at 20 mA and 15 kV. ^{31}P and ^{27}Al MAS NMR measurements were carried out using a Bruker ASX 300 spectrometer at 121.44 and 78.16 MHz frequencies, respectively, at room temperature. ^{31}P MAS NMR spectra were obtained using a 90° pulse with duration 3.2 μs, relaxation time 60 s, and spinning rate 4 kHz, and chemical shifts were referred to external H_3PO_4 (85%) solution. ^{27}Al MAS NMR spectra were obtained with 4 kHz spinning rate using 90° pulse with duration 0.7 μs and recycle delay 0.5 s. A solution of aluminum nitrate with pH ≈ 1 was used as an external reference. Spinning side bands were confirmed by changing the spinning rate.

Catalytic Oxygenation with H_2O_2

All catalytic oxygenation runs were carried out in a glass reactor equipped with a reflux condenser, a magnetic stirrer, and a gas burette to monitor possible molecular oxygen evolution.

In a typical experimental procedure 200 mg catalyst was mixed with 10 g reactant in a glass reactor, 5 g acetone was used as solvent and the mixture heated to the reaction temperature (350 K) under constant stirring. Reaction temperature was maintained using a temperature-controlled water bath. Then 0.0882 mol H_2O_2 (30% aqueous solution) was slowly added into the reactor.

Samples were taken at regular intervals and analyzed using a gas chromatograph (HP 5890) equipped with a 30-m capillary (DB-Wax) column and flame ionization detector (FID). The identity of the products was verified from retention times of pure compounds. H_2O_2 decomposition and consumption were also monitored using a gas collector and iodometric titration, respectively.

A special kind of experiment was performed with the purpose of checking the possibility of hypothetical leached Ti species to be active in the oxidation process. Thus an experiment performed under the above-described conditions was interrupted after 3 h. The hot two-phase liquid medium sucked with syringe equipped with a filter and immediately transferred to another reactor already at the same temperature. The compositions of the two phases were then monitored for another 2 h.

High-purity (Aldrich Chemical Co.) Cyclohexane, *n*-hexane, cyclohexanol, hexanol-2, cyclohexene, and octene-1 were used as substrates for oxidation and epoxidation reactions.

RESULTS AND DISCUSSION

Characterization

From XRD results it was found that all TAPO samples are very well crystallized and no crystalline phase impurity was observed. The elemental chemical analyses of TAPOs and their AlPOs analogs are presented in Table 1. Upon comparing TAPO's data with the composition of AlPO samples prepared under similar conditions, it was suggested that in TAPO-5 titanium substitutes P atoms, whereas in TAPO-11 and TAPO-36, it substitutes Al + P pairs. These two mechanisms of Ti substitution are similar to those reported for Si incorporation in silico-aluminophosphate molecular sieves (17).

Diffuse reflectance UV–vis spectra of the three TAPOs (Fig. 1) showed a maximum at 230–240 nm with a shoulder at 280 nm. For comparison the DRS UV–vis spectrum of anatase is also displayed in inset of Fig. 1. A broad absorption signal with a maximum at about 328 nm is characteristic of this oxide. The absence of any shoulder at 330–350 nm in DRS UV–vis spectra of three TAPOs suggests that all samples are free from extraframework anatase like titanium oxide. However, the shoulder at 280 nm can be attributed to framework-linked Ti atoms with octahedral symmetry or to a very small amount of highly dispersed extraframework oligomers (di- and/or trimers) TiO_2 species. Similar DRS UV–vis spectra for example have been reported for some titanosilicate mesoporous molecular sieves samples by Franke *et al.* (21). These authors concluded that titanium was incorporated in the titanosilicate framework. Moreover no titanium oxides species were detected by Raman spectroscopy in TAPO samples with similar DRS UV-vis spectra (13). In addition our BET and *n*-butane adsorption results (Table 1) support the absence of significant oxide debris inside micropores.

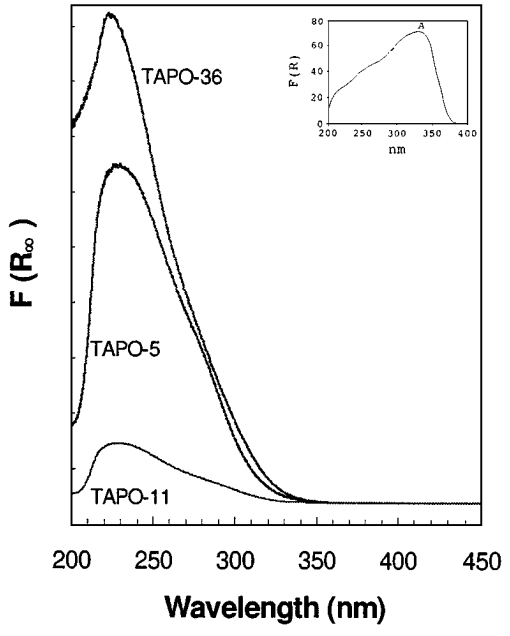

FIG. 1. Diffuse reflectance UV–vis spectra of TAPOs and anatase (inset).

TABLE 2

Summary of XPS Data (BE Referenced to $C_{1s} = 284.6$ eV)

	Surface composition (atom%)			Binding energies (eV)		
	Al	P	Ti	Al_{2p}	P_{2p}	$Ti_{2p3/2}$
TAPO-5	0.54	0.40	0.06	75.3	134.7	458.8
AlPO-5	0.52	0.48	—	75.1	134.5	—
TAPO-11	0.57	0.40	0.03	75.0	134.5	458.2
AlPO-11	0.52	0.48	—	74.9	134.5	—
TAPO-36	0.58	0.38	0.04	74.9	134.7	459.0
AlPO-36	0.54	0.46	—	—		—

XPS binding energies and apparent relative atomic concentrations of Al, P, and Ti in TAPO samples are summarized in Table 2. The binding energy of $Ti_{2p3/2}$ in TAPOs is systematically higher than the value (457.8–458.0 eV) which is accepted for octahedral Ti^{4+}, and interestingly this difference is more pronounced for TAPO-36 sample with higher titanium content compared to the other two.This indicates that the Ti^{4+} ions by XPS are not octahedrally coordinated anatase-like extraframework. The Al surface concentration was found to be higher compared to that of the bulk in all TAPO samples. Similar observations were also made for the AlPO analogs. This could be interpreted as indicating an Al-enriched external surface of the TAPO particles. It should be recalled, however, that because of the very small depth of analysis of XPS, this may correspond to a very minor deviation from the stoechiometry for the above particles. The surface concentration of Ti is either equal to or slightly higher than the bulk values reported in Table 1.

^{31}P and ^{27}Al MAS NMR spectra of calcined and air-exposed TAPOs with their AlPOs counterparts are presented in Fig. 2. From ^{27}Al peak position of all TAPOs it is obvious that aluminium is present in tetrahedral environment and no additional peaks or broad-line features due to octa- or penta-coordinated Al species are observed. Only in $AlPO_4$-11 is a peak at about −15 ppm attributed to octahedral Al species which may be due to extraframework material as confirmed by the low BET surface area observed for this sample (see Table 1). Similar conclusions are made from the ^{31}P NMR spectra. A single ^{31}P band is observed at −27.4 to −29.9 ppm and assigned to

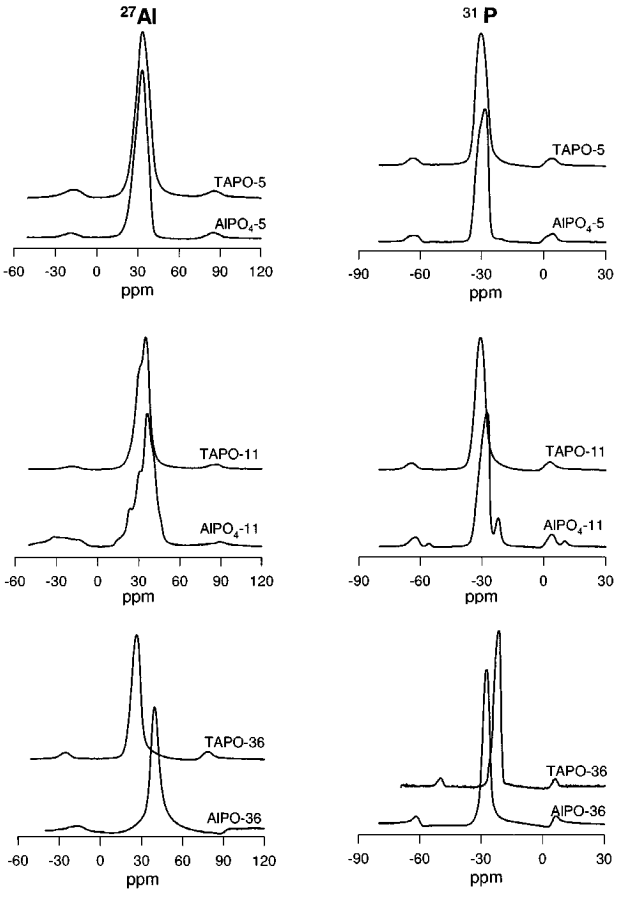

FIG. 2. ^{27}Al and ^{31}P MAS NMR spectra of TAPOs and their AlPO analogs.

framework tetrahedral phosphorous. In $AlPO_4$-11, a second peak at −22.9 ppm is ascribed to partly hydrolyzed tetrahedral phosphorous (22), which could be present in extraframework material.

Thus our data on XRD, DRS UV–vis, BET surface area, *n*-butane adsorption, XPS, and ^{31}P and ^{27}Al MAS NMR all indicate that the TAPO samples are well crystallized and essentially free from extraframework species. From the decrease in unit cell parameters upon Ti incorporation reported in Ref. (15) it was concluded that Ti is in lattice position. The exact environment of Ti in all TAPOs is not yet fully known. In a recent paper, Prakash *et al.* (23) studied by ESR and electron spin echo modulation (ESEM) the environment of Ti in TAPO-5. They concluded that Ti substitutes framework P in this material, which is in line with our suggestions (15). Moreover the investigation by XANES and EXAFS of our TAPO samples (24) indicates that the Ti environment is essentially the same for TAPO-5, -11, and -36 and quite different from the one in Ti-silicalites. However, the presence of dimeric Ti species substituting for Al and P pairs in TAPO-11 and TAP-36, must not be considered definitively established. Further work aiming at this clarification is in progress in our laboratory.

Catalytic Measurements

Oxidation of cyclohexane. Cyclohexane oxidation was carried out at 350 K over the three titanium aluminophosphate molecular sieves. The results are summarized in Table 3. For comparison the results of a similar test performed using TS-1 as the catalyst are also included. In

TABLE 3

Cyclohexane Oxyfunctionalization on Titanium Aluminophosphate Molecular Sieves of AFI, AEL, and ATS Type

Catalyst	Reaction time (h)	Cyclohexane conversion (%)	Average reaction rate (mol m^{-2} h^{-1})	H_2O_2 Conversion[a] (%)	H_2O_2 Selectivity[b] (%)	Product distribution Cyclo-hexanone (%)	Product distribution Cyclo-hexanol (%)	ol/one ratio
TAPO-5	1	1.4	1.46e-5	3.9	48.7	3.2	96.8	30.2
	3	2.5		6.7	51.1	6.2	93.8	15.2
	5	4.4		11.3	52.0	8.1	91.9	11.4
TAPO-11	1	1.4	1.19e-5	4.5	43.1	10.5	89.5	8.6
	3	2.3		7.0	44.5	11.3	88.7	7.9
	5	4.2		13.2	42.5	10.7	89.4	8.4
TAPO-36	1	0.9	1.12e-5	4.6	27.5	16.1	83.9	5.2
	3	2.0		9.0	30.6	12.0	88.0	7.4
	5	3.7		14.7	34.0	13.0	87.1	6.7
TS-1	1	1.9	1.36e-5	4.0	65.9	4.8	95.2	20.0
	3	4.2		8.3	66.1	9.1	90.9	10.0
	5	6.3		13.1	64.9	18.6	81.4	4.3

[a] H_2O_2 selectivity: H_2O_2 utilized for oxyfunctionalization products/H_2O_2 overall consumption.
[b] H_2O_2 conversion: H_2O_2 overall consumption/H_2O_2 initially introduced.

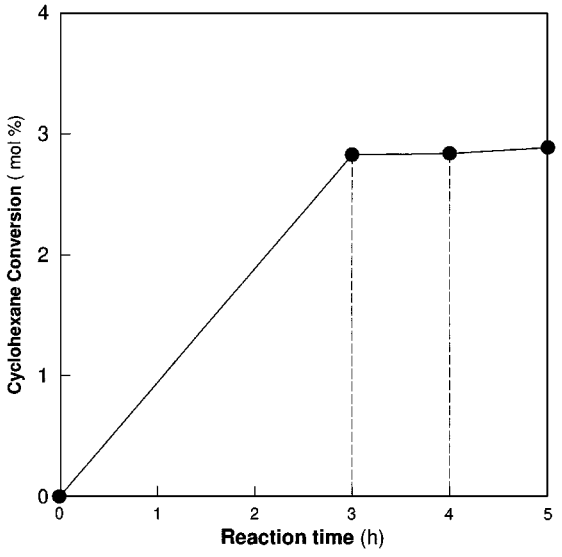

FIG. 3. Activity of reaction solution with TAPO-5 (up to 3 h) and after TAPO-5 removal (3–5 h).

all cases the only products detected were cyclohexanol and cyclohexanone. The selectivity to cyclohexanol was very high. The cyclohexane conversions and H_2O_2 selectivities were found to be in the order TS-1 > TAPO-5 > TAPO-11 > TAPO-36, which is essentially the same as for specific surface areas (see Table 1). It is noteworthy that both TAPO-5 and TAPO-11 show activities and selectivities only slightly lower than TS-1. It must be emphasized that titanium silicalites (and Ti-β) are the only known catalysts to be active for alkanes oxyfunctionalization under such conditions.

The lower H_2O_2 selectivity observed on the TAPO samples suggests higher contents of extraframework Ti in these samples. Attempts were also made at performing *n*-hexane and cyclohexane oxidations at lower temperatures (~328 K). Under these conditions no reactivity could be measured for any of the three TAPO samples, whereas TS-1 showed already significant oxidation rates. That no considerable catalytic activity is observed in TAPOs at this temperature may be attributed to the lower rate of reaction inside the relatively hydrophilic channels of AlPOs compared to those of hydrophobic TS-1. No test of *n*-hexane reaction can be tried at 350 K since this is above *n*-hexane normal boiling point.

In some recently published literature (7, 25) it was reported that the activity of V- and Cr-aluminophosphate molecular sieves in liquid-phase oxidation reactions was due to minor amounts of metal leached out of the solid catalyst and present in the reaction solution. We have found no activity of liquid phase alone after filtering out TAPO catalyst from reaction media (see Experimental). Figure 3 shows the result of such a reaction test performed with TAPO-5 catalyst. It is evident that no hypothetical Ti species leached out of TAPOs was responsible for the observed catalytic activity since the oxidation reaction was stopped after catalyst removal. In another separate test a blank reaction was performed under the same condition using $AlPO_4$-5 molecular sieve. No catalytic activity has been observed after 6 h. From these two reaction tests it is concluded that the activity of TAPO catalyst can be only due to Ti atoms substituted in the framework of aluminophosphate molecular sieves.

Oxidation of alcohols and cyclo-alcohols. As is shown in Tables 4 and 5, TAPOs are also capable of catalyzing the oxidation of alcohols and cyclo-alcohols at 350 K. From hexanol-2 and cyclohexanol only hexanone-2 and cyclohexanone were obtained, respectively. Again compared to titanium silicalite, the TAPOs showed a lower activity and H_2O_2 selectivity. Particularly TAPO-36 exhibited a nearly 50% drop in activity and H_2O_2 selectivity compared to TS-1 under similar reaction conditions. Moreover, the order of oxidation activity as well as H_2O_2 selectivity were similar to the ones observed in cyclo-hexane oxyfunctionalization (Table 3).

Epoxidation of alkenes and cyclo-alkenes. The activity of TAPOs in these epoxidations was again found to be only slightly below that of Ti-silicalite. In general, the only product formed was 1,2-epoxyoctane or cyclo-epoxyhexane for the epoxidation of 1-octene and cyclo-hexene, respectively (Tables 6 and 7). No other side product was observed. A relatively lower H_2O_2 decomposition to molecular oxygen was obtained as compared to the other oxidation reactions studied.

In the literature it has been often reported that over titanium silicalites the rate of olefins epoxidation was significantly higher than the rates of alkane oxyfunctionalization. The difference was the basis for assuming different reaction mechanisms for the two kinds of oxidation reactions (18). It is thus of interest to note here that also with the TAPO catalysts, epoxidation seems to be a faster and more selective reaction than alkanes or alcohols oxidations.

H_2O_2 decomposition. A fair activity for H_2O_2 decomposition to molecular oxygen and water was indeed observed over these TAPO samples. The decomposition mentioned by the volume of oxygen gas generated as a function of time appeared to be higher with TAPO-36, while the order of H_2O_2 decomposition was TAPO-36 > TAPO-11 > TAPO-5 > TS-1.

The nonframework titanium usually effectively catalyzes the H_2O_2 decomposition reaction, which is likely associated with low coordination surface titanium sites in this material. The DRS–UV–vis spectra of these three TAPO samples (Fig. 1) also suggest the presence of titanium in low coordination, since no absorption band centered at 330 nm corresponding to anatase was observed.

Some blank experiments performed in identical reaction conditions using 200 mg high surface area anatase

TABLE 4

Cyclohexanol Oxidation Activity on Titanium Aluminophosphate Molecular Sieves of AFI, AEL, and ATS Type

Catalyst	Reaction time (h)	Average reaction rate (mol m^{-2} h^{-1})	Cyclohexanol conversion (%)	H_2O_2 Conversion[a] (%)	H_2O_2 Selectivity[b] (%)
TAPO-5	1	1.43e-5	1.5	4.5	37.1
	3		3.5	10.4	38.5
	5		5.0	15.0	38.0
TAPO-11	1	1.29e-5	1.2	5.0	26.3
	3		3.3	12.1	31.1
	5		4.8	17.3	31.5
TAPO-36	1	1.01e-5	0.9	5.4	19.1
	3		2.6	13.3	22.3
	5		3.9	18.8	23.6
TS-1	1	1.48e-5	2.4	4.0	68.6
	3		5.0	9.2	61.7
	5		8.1	14.9	61.2

Note. Product selectivity for cyclo-hexanone is 100% for all catalysts.
[a] H_2O_2 selectivity: H_2O_2 utilized for oxidation products/H_2O_2 overall consumption.
[b] H_2O_2 conversion: H_2O_2 overall consumption/H_2O_2 initially introduced.

(225 m^2/g) are reported in Table 8. In these tests no oxidation products were detected but the rate of H_2O_2 decomposition could be monitored by measuring the volume of the molecular oxygen gas generated as a function of reaction time. It is seen from these results that the surface sites of anatase are highly active in H_2O_2 decomposition. The slightly lower decomposition rates observed during olefin epoxidations may be associated with a better competition of the olefins for adsorption on these active sites.

All results for the number of moles of oxygenates produced after 5 h reaction are presented in Fig. 4 for the five substrates studied. The results for H_2O_2 selectivity in the same experiments are given in Fig. 5. These two figures show first that the order of activities and H_2O_2 selectivities over

TABLE 5

Oxidation of Hexanol-2 on Titanium Aluminophosphate Molecular Sieves of AFI, AEL, and ATS Type

Catalyst	Reaction time (h)	Average reaction rate (mol m^{-2} h^{-1})	Hexanol-2 conversion (%)	H_2O_2 Conversion[a] (%)	H_2O_2 Selectivity[b] (%)
TAPO-5	1	1.45e-5	1.2	3.3	39.5
	3		3.0	8.6	39.0
	5		4.8	13.1	40.5
TAPO-11	1	1.05e-5	1.2	4.1	33.4
	3		2.9	9.7	32.9
	5		4.2	13.8	33.4
TAPO-36	1	7.88e-6	0.8	4.5	18.9
	3		2.3	10.5	24.3
	5		3.2	14.2	25.1
TS-1	1	1.45e-5	2.0	4.1	55.6
	3		4.6	9.3	55.4
	5		7.7	15.6	54.8

Note. Product selectivity of hexanone-2 is 100% for all catalysts.
[a] H_2O_2 selectivity: H_2O_2 utilized for oxyfunctionalization products/H_2O_2 overall consumption.
[b] H_2O_2 conversion: H_2O_2 overall consumption/H_2O_2 initially introduced.

TABLE 6

Catalytic Epoxidation of Octene-1 on Titanium Aluminophosphate Molecular Sieves of AFI, AEL, and ATS Type

Catalyst	Reaction time (h)	Average reaction rate (mol m^{-2} h^{-1})	Octene-1 conversion (%)	H_2O_2 Conversion[a] (%)	H_2O_2 Selectivity[b] (%)
TAPO-5	1	1.94e-5	1.9	3.5	55.5
	3		3.9	7.2	54.6
	5		7.2	13.3	54.4
TAPO-11	1	1.50e-5	1.4	3.4	42.1
	3		3.1	7.6	41.6
	5		6.1	14.4	42.7
TAPO-36	1	1.11e-5	1.2	3.6	32.5
	3		2.2	7.2	30.9
	5		4.9	15.1	32.6
TS-1	1	1.88e-5	2.9	3.9	74.5
	3		7.0	9.5	74.2
	5		11.0	15.2	73.1

Note. Product selectivity of 1,2 epoxyoctane is 100% for all catalysts.
[a] H_2O_2 selectivity: H_2O_2 utilized for epoxidation products/H_2O_2 overall consumption.
[b] H_2O_2 conversion: H_2O_2 overall consumption/H_2O_2 initially introduced.

the four catalysts in oxygenation reactions is unchanged with the substrate. In addition Fig. 4 reveals that the two epoxidation reactions are faster than the other three oxidations whatever the catalyst. This suggests that the same sites are active in all these five reactions and that the three TAPO samples contain lower numbers of these active sites per unit mass than the TS-1 sample. A lower H_2O_2 selectivity means a higher rate of H_2O_2 decomposition yielding molecular oxygen. These results in Fig. 5 thus suggest that the TAPOs contain higher amounts of low coordinated surface titanium in extraframework material than the TS-1 sample.

It is interesting to note that the order of activity is not related to the order of pore size. The TS-1 sample which has the smallest pore aperture is also the most active. This observation suggests that the reactions under study are not limited by internal diffusion in any of the TAPO samples.

TABLE 7

Cyclohexene Epoxidation on Titanium Aluminophosphate Molecular Sieves of AFI, AEL, and ATS Type

Catalyst	Reaction time (h)	Average reaction rate (mol m^{-2} h^{-1})	Cyclohexene conversion (%)	H_2O_2 Conversion[a] (%)	H_2O_2 Selectivity[b] (%)
TAPO-5	1	2.33e-5	2.0	4.4	62.8
	3		4.1	17.6	63.9
	5		7.8	33.1	65.5
TAPO-11	1	1.82e-5	1.5	4.0	52.0
	3		3.7	19.8	52.4
	5		6.7	35.0	52.9
TAPO-36	1	1.41e-5	1.2	3.9	42.0
	3		3.0	19.0	43.6
	5		5.5	35.6	43.0
TS-1	1	2.09e-5	3.3	5.8	79.5
	3		7.6	26.2	79.3
	5		11.5	41.5	76.4

Note. Product selectivity of cyclo-epoxyhexane is 100% for all catalysts.
[a] H_2O_2 selectivity : H_2O_2 utilized for epoxidation products/H_2O_2 overall consumption.
[b] H_2O_2 conversion : H_2O_2 overall consumption/H_2O_2 initially introduced.

TABLE 8

Catalytic Decomposition of H_2O_2 over High-Surface Area Anatase in the Presence of Different Substrates[a]

Substrate	Reaction time (h)	O_2 gas (mol)	H_2O_2 conversion (%)
Cyclohexane	1	0.00904	10.2
	3	0.01608	18.2
	5	0.02496	28.3
Cyclohexanol	1	0.00992	11.2
	3	0.02056	23.3
	5	0.02616	29.5
Hexanol-2	1	0.01048	11.9
	3	0.02256	25.7
	5	0.02936	33.3
Cyclohexene	1	0.00736	8.34
	3	0.01376	15.6
	5	0.02088	23.7
1-Octene	1	0.00872	9.9
	3	0.01568	17.8
	5	0.02416	27.4

[a] Reaction carried out at 350 K with 200 mg anatase, 10 g substrate, 0.0882 mol H_2O_2, and 5 g acetone (solvent).

Previous work (26, 27) in our laboratory has indeed shown that with both TS-1 and TS-2 catalysts diffusional effects are not significant in the conversion of *n*-hexane under similar conditions.

CONCLUSIONS

The significant result of the present work is that framework tetrahedral titanium sites having catalytic properties comparable to the properties of similar sites in Ti-silicalites can be accommodated in several AlPO lattices. This indeed opens a new perspective in the preparation of zeolite oxydo-reduction catalysts useful in reactions with diluted hydrogen peroxide. The wide diversity of AlPO crystalline structures may therefore be explored as potential hosts for active titanium sites. Many large-pore AlPO may provide new possibilities for oxidation of larger molecules by H_2O_2 or by larger organic peroxides such as *t*-butyl hydroperoxide or cumene hydroperoxide.

In the interpretation of the special properties of titanium silicalites as oxidation catalysts some authors emphasize the relative hydrophilicity of the silicalite structure (20). It is therefore potentially important that AlPO literature describe some samples of AlPO-5 and AlPO-31 as quite hydrophobic materials (17). Thus the AlPO family may provide environments for the Ti cations with a variety of hydrophobic properties.

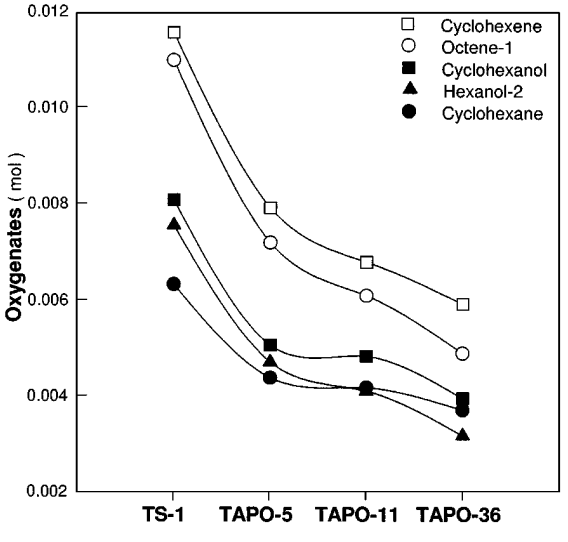

FIG. 4. Oxygenates production with different substrates after 5 h over TAPOs and TS-1.

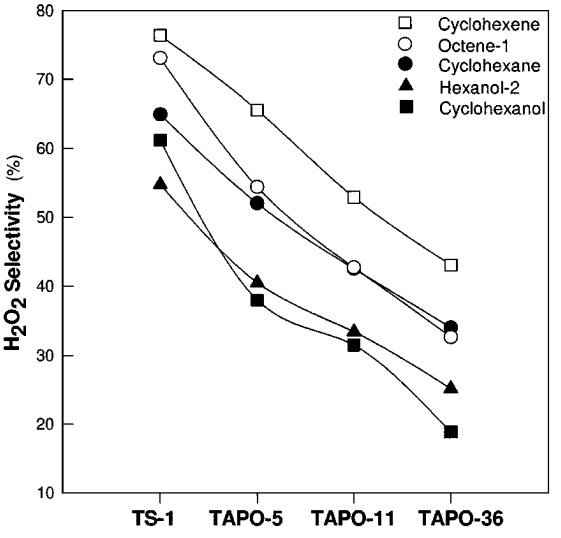

FIG. 5. H_2O_2 selectivity for different substrates after 5 h over TAPOs and TS-1.

REFERENCES

1. Wilson, S. T., Lok, B. M., Messina, C. A., Cannan, T. R., and Flanigen E. M., *J. Am. Chem. Soc.* **104**, 1146 (1982).
2. Meier, W. M., Olson, D. H., and Baerlocher, Ch., "Atlas of Zeolite Structure Types," Elsevier, Amsterdam/New York, 1996.
3. Taramasso, N., Perego, G., and Notari, B., U.S. Patent 4410501 (1983).
4. Reddy, J. S., and Kumar, R., *Zeolites* **12**, 95 (1992).
5. Camblor, M. A., Corma, A., and Perez-Pariente, *Zeolites* **13**, 82 (1992).
6. Rigutto, M. S., and van Bekkum, *J. Mol. Catal.* **81**, 77 (1993).
7. Chen, J. D., Dakka, J., and Sheldon, R. A., *Appl. Catal.* **108**, L1 (1994).
8. Dai, P. E., Petty, R. H., Ingram, C. W., and Szostak, R., *Appl. Catal. A* **143**, 101 (1996).
9. Haanepen, M. J., and van Hoof, J. H. C., *Appl. Catal. A* **152**, 183 (1997).
10. Luna, F. J., Ukawa, S. E., Wallau, M., and Schuchardt, U., *J. Mol. Catal.* **117**, 405 (1997).
11. Lok, B. M., Marcus, B. K., and Flanigen, E. M., U.S. Patent 4500651 (1985).
12. Zahedi-Niaki, M. H., Joshi, P. N., and Kaliaguine, S., *J. Chem. Soc. Chem. Commun.*, 47 (1996).

13. Ulagappan, N., and Krishnasamy, V., *J. Chem. Soc. Chem. Commun.*, 373 (1995).
14. Zahedi-Niaki, M. H., Joshi, P. N., and Kaliaguine, S., *J. Chem. Soc. Chem. Commun.*, 1373 (1996).
15. Zahedi-Niaki, M. H., Joshi, P. N., and Kaliaguine, S., *in* "Proceedings on the 11th International Zeolites Conference" (H. Chon, S.-K. Ihm, and Y. S. Uh, Eds.), p. 1013. Elsevier, Amsterdam, 1997.
16. Akolekar, D. B., and Ryong, R., *J. Chem. Soc. Faraday Trans.* **92**, 4617 (1996).
17. Flanigen, E. M., Patton, R. L., and Wilson, S. T., *Stud. Surf. Sci. Catal.* **37**, 13 (1988).
18. Khouw, C. B., Dartt, C. B., Labinger, J. A., and Davis, M. E., *J. Catal.* **149**, 195 (1994).
19. Wilson, S. T., Lok, B. M., Messina, C. A., and Flanigen, E. M., *in* "Proceedings on the 6th International Zeolites Conference" (D. Olson and A. Bisio, Eds.), p. 97. Butterworth, Guildford, Surrey, UK, 1983.
20. Sheldon, R. A., and Dakka, *J. Catal. Today* **19**, 215 (1994).
21. Franke, O., Rathousky, J., Schulz-Ekloff, G., Starek, J., and Zukal, A., *in* "Proceedings on the 11th International Zeolites Conference" (H. Chon, S.-K. Ihm, and Y. S. Uh, Eds.), p. 77. Elsevier, Amsterdam, 1997.
22. Mikhailenko, S. D., Zaidi, J., and Kaliaguine, S., *J. Chem. Soc. Faraday Trans.*, in press.
23. Prakash, A. M., Kurshev, V., and Kevan, L., *J. Phys. Chem. B* **101**, 9794 (1997).
24. Zahedi-Niaki, M. H., Beland, F., Bonneviot, L., and Kaliaguine, S., in preparation.
25. Lempers, H. E. B., and Sheldon, R. A., *Stud. Surf. Sci. Catal.* **105B**, 1061 (1997).
26. Gallot, J. E., Do Trong, O., Kapoor, M. P., and Kaliaguine, S., *Ind. Eng. Chem. Res.* **36**, 3458 (1997).
27. Fu, H., and Kaliaguine, S., *J. Catal.* **148**, 540 (1994).